Characterization of Jovian Plasma-Embedded Dust Particles

Amara L. Graps

INAF Istituto di Fisica dello Spazio Interplanetario, CNR-ARTOV, Via del Fosso del Cavaliere 100, 00133 Rome, Italy. Fax: +39-06-4993-4383

Abstract

As the data from space missions and laboratories improve, a research domain combining plasmas and charged dust is gaining in prominence. Our solar system provides many natural laboratories such as planetary rings, comet comae and tails, ejecta clouds around moons and asteroids, and Earth's noctilucent clouds for which to closely study plasma-embedded cosmic dust. One natural laboratory to study electromagnetically-controlled cosmic dust has been provided by the Jovian dust streams and the data from the instruments which were on board the Galileo spacecraft. Given the prodigious quantity of dust poured into the Jovian magnetosphere by Io and its volcanoes resulting in the dust streams, the possibility of dusty plasma conditions exist. This paper characterizes the main parameters for those interested in studying dust embedded in a plasma with a focus on the Jupiter environment. I show how to distinguish between dust-in-plasma and dusty-plasma and how the Havnes parameter P can be used to support or negate the possibility of collective behavior of the dusty plasma. The result of applying these tools to the Jovian dust streams reveals mostly dust-in-plasma behavior. In the orbits displaying the highest dust stream fluxes, portions of orbits E4, G7, G8, C21 satisfy the minimum requirements for a dusty plasma. However, the P parameter demonstrates that these mild dusty plasma conditions do not lead to collective behavior of the dust stream particles.

Key words: charged dust, Jovian dust streams, dusty plasma, Jovian magnetosphere, Havnes parameter, Debye length, Galileo mission

1 Introduction

As the data from space missions and laboratories improve, a research domain combining plasmas and charged dust is gaining in prominence. Our universe is comprised of 99% plasma, and cosmic dust is ubiquitous, yet a discussion of the in-

Email address: `amara.graps@ifsi-roma.inaf.it` (Amara L. Graps).

Preprint submitted to Planetary and Space Science – special issue

terplay between the two is often missing from the astrophysics textbooks. Our solar system provides many natural laboratories such as planetary rings, comet comae and tails, ejecta clouds around moons and asteroids, and Earth's noctilucent clouds for which to closely study plasma-embedded cosmic dust. After the Voyager spacecraft(s) left the giant planets, and the spacecraft flotilla studying comet Halley went their own way too, one space laboratory for studying dust-embedded-in-plasma appeared upon the arrival of the Galileo spacecraft into the Jupiter magnetosphere. The spacecraft carried an impact ionization dust instrument (Dust Detector Subsystem or DDS) to sample in-situ the dust particles, and, combined with the plasma instruments, an eight-year (1996-2003) mission, and a strong dust source of the moon Io, from which material escapes at an approximate rate of 1 ton sec^{-1} (Spencer and Schneider, 1996), the potential to study dusty plasmas was enormous.

This paper characterizes the main parameters for those interested in studying dust embedded in a plasma with a focus on the Jupiter environment. I start with mathematical descriptions to aid one in distinguishing between different dust-in-plasma regimes, I apply these terms for the Jovian dust streams in order to identify in which regions of the Jovian magnetosphere I might see collective dust particle behavior, and then I apply these parameters. This Jovian dust data comprises one population of several different Jovian populations. The Jovian dust streams are high-rate bursts of fast (at least 250 km-sec^{-1}) submicron-sized particles from Jupiter's moon Io, in particular, dust from Io's volcanoes (Graps et al., 2000). The plasma parameters used in the subsequent tables were mostly derived from a model of the Jovian plasma.

To describe the dust particles' physical behavior, one must identify the involved forces. The intermediate force range between gravitationally-dominated dust stream particles and electrodynamically-dominated ions and electrons is the regime where dust particles lie. Charged cosmic dust dynamics brings both forces into play: particles typically micron-sized and larger are dominated by gravity, while submicron-sized particles are progressively dominated by electromagnetism (the Lorentz force), as their sizes decrease. In order to quantify possible collective effects, I must characterize *both* the Jovian plasma and the dust streams particles, deriving their interparticle distances, energies, and dynamics.

In dust-plus-plasma mixtures, there are three characteristic length scales: 1) the dust grain size a, the 2) the plasma Debye length λ_D, and 3) an average intergrain distance d, which is equal to the dust number density n_d by $n_d d^3 = 1$. In order to determine whether collective processes are important, I use these length scales to compare plasma-plus-dust regimes and for additional information, I calculate the Havnes parameter P (Verheest, 2000; Goertz, 1989; Havnes et al., 1987), which is the ratio of dust charge density to the electron charge density, given by $Z_d n_d / n_e$, where n_e is the electron density and Z_d is the dust particle charge number $|\mathrm{Q}| / e$) for the same conditions.

The Debye screening length, λ_D provides our first indication whether collective processes might be important. The Debye length is the distance over which the

Coulomb field of an arbitrary charge in the plasma is shielded. If the mean separation between the dust particles in the plasma d is smaller than the Debye length, then neighboring charged dust particles are not shielded and isolated from each other, and they begin to act like a solid dielectric (Cravens, 1997, pg. 35).

Proceeding further to characterize collective processes. In the dust-plus-plasma mixture, I can have two regimes depending on the concentration of the dust grains: (Verheest, 2000, Pg. 5-6)

- ‘Dust-in-Plasma’: If $a \ll \lambda_D < d$, then I have a plasma containing isolated screened dust grains and can treat the dust from a particle dynamics point of view.
- ‘Dusty Plasma’: If $a \ll d < \lambda_D$, then collective effects of the charged dust can be relevant.

Verheest (2000) describes the complex charging of dust in a dusty plasma. If the dust density in the plasma is increased, with an inverse effect on the average distance d between the grains, the equilibrium charge on the particles decreases dramatically, and two effects play a role in opposite directions (Verheest, 2000; Goertz, 1989): grain capacitance increases, and each grain does not have to become so negative (or positive), in order to equalize the ion (or electron) currents to its surface.

The Jupiter’s plasma discussed here, and in my dust stream dynamics calculations is a fit by M. Horányi to the Voyager 1 and 2 cold plasma measurements described in Bagenal (1989). Horányi assumed a constant mixing ratio of 1:2 of singularly ionized oxygen to sulphur ions. The plasma is quasi-neutral, i.e. $n_i = n_e$. I selected particular locations: 6.2, 8, 10, 15, 20, 30 R_{J} (R_{J} = radial distance 71492 km from the center of Jupiter) and present them in Table 1. These particular locations, and Table 1
temperatures (T_e and T_i, respectively), electron density (n_e), and average ion mass numbers (avim in a.m.u.) will be used again in subsequent tables.

In the following text, I provide equations (SI units) for the individual particle (electrons, ions, dust particles) motions of the dust-plus-plasma, for bulk motions of the plasma, and tables of the values for the plasma model.

2 Single Particle Motion

In a constant magnetic vertical field B_z, the motion of an individual, charged particle (electron, ion, tiny dust particle) is a helix of constant pitch around magnetic field lines. For this particle, the vertical velocity component v_z is unaffected by B, while the rotational velocity component: v_θ (=$\sqrt{v_x^2 + v_y^2}$), is constant and gives the circular motion about the center of the orbit. Then:

$$qv_\theta B = \frac{m_{(i,e,d)} v_\theta^2}{R_g} \quad , \quad R_g = \frac{m_{(i,e,d)} v_\theta}{qB} \quad . \tag{1}$$

where q is the charge of the particle, v_θ (=$\sqrt{v_x^2 + v_y^2}$) is the rotational velocity component, $m_{i,e,d}$ is its mass (where the subscript refers to either ions, electrons or dust particles), and R_g is its gyroscopic radius. The gyroscopic radius can be associated with the temperature T of the particle by using the thermal kinetic energy. Since v_z is unaffected by B, the rotational velocity is:

$$v_\theta = \sqrt{\frac{2k_BT}{m_{(i,e,d)}}} \quad , \tag{2}$$

where k_B is the Boltzmann constant. Then the root-mean-squared gyroscopic radius in terms of temperature is:

$$R_g = \frac{1}{qB}\sqrt{2m_{(i,e,d)}k_BT} \quad . \tag{3}$$

Note that the thermal energy of the particle becomes a part of two constants of the motion: the total (vertical and rotational) kinetic energy $\frac{1}{2}(m\vec{v})$, and the magnetic moment: $(1/2)(mv_\theta^2)/B$, since v_z, v_θ and the mass of the particle is constant. The vertical velocity and hence its motion enters via $v_z = \sqrt{(2/m)(W - \Phi)}$, where W equals the total energy and Φ is the potential energy. An exploration of the transfer of vertical kinetic energy in the context of charged particles trapped in a drift tube is in Graps (1991).

Another useful expression for the gyroradius is in terms of the gyrofrequency (also called cyclotron frequency or Larmor frequency):

$$R_g = \frac{v_\theta}{\Omega_{(i,e,d)}} \quad , \tag{4}$$

where the magnitude of the gyrofrequency Ω for ions, electrons and dust in SI units (Cravens, 1997, pg. 44) is:

$$\Omega_{i,e,d} = \frac{qB}{m_{(i,e,d)}} \quad (\mathrm{radians} - \mathrm{s}^{-1}). \tag{5}$$

For these purposes, I can consider a dipole for Jupiter's magnetic field, $B = B_0(R_\mathrm{J}/r)^3$, where B_0 = 4.28 G is the field strength at the equator at Jupiter's surface (R_J), and r = the radial distance from the center of Jupiter.

In Table 2, I list ion, electron and electron velocities, and dust sizes, charges, velocities (average: $\langle v \rangle = v_\theta$), or speeds for the single particles. For the ions and electrons, the velocities were calculated from the thermal kinetic energy (Eqn. 2), given the masses (m_i, m_e) and the ion and electron temperatures (T_i, T_e) listed in Table 1. These same parameters for the dust particles were gained by a different method. Table 2

The Galileo DDS did not measure the dust particle charge directly, but measured, instead, an impact plasma that depended on the particle's velocity and mass, upon

which laboratory calibrations were applied. Therefore, for the dust particles' sizes, charges, and velocities, I relied on the dust streams model in Graps (2001) to determine these properties indirectly. Investigators since 1995 (Grün et al., 1996a,b, 1997; Horányi et al., 1997; Graps, 2001; Krüger et al., 2003), have best matched the fluxes or dynamics of the Jovian dust streams with a (seven free parameters) model that includes electron and ion collection currents as well as photoelectron emission and secondary electron emission currents. These currents were integrated to determine the particle's charge simultaneously with the particle's dynamics. To generate average particle properties throughout the Jovian magnetosphere, I launched 287200 trajectories at Keplerian speeds from a ring just outside Io's orbit at 6.2 R_{J}, and stopped the simulation after fifteen hours of dust particle travel time. The particles that remained inside of the magnetosphere, I then considered to be representative for many parameters of interest (with the exception of number density) of the general population of Jovian dust stream particles within 50 R_{J}. For each dust particle trajectory, I choose randomly between a minimum and maximum value for the free parameters: 1) spherical particle density and radius, 2) radiation pressure scattering coefficient, 3) photoelectric yield for the photoelectron emission current and the energy (Maxwellian) distribution of photoelectrons released from grain when a photon impacts onto the dust particle, 4) maximum yield of secondary electrons released by a high energy impacting electron or ion, and 5) orbital phase, 6) magnetic field orientation, and 7) initial dust charge. Figure 1 displays the simulation output for the dust particles' charge potential, radii, and speeds. Then to calculate the averages seen in Table 2, I sliced ($\pm$ 0.1 R_{J}) through the radial locations: 6.2, 8, 10, 15, 20, and 30 R_{J}. for the particles' sizes, charges and speeds. Figure 1

In Table 3, I list gyrofrequencies calculated from Eqn. (5), which includes a constant magnetic field, and gyroradii calculated from Eqn. (4) for ion, electron, and dust particles. Table 3

3 Towards Collective Particle Motions

Collective interactions occur when self-generated fields of the particles take over a correlative role in scattering the electrons (Baumjohann and Treumann, 1997, Pg. 72). The Debye screening length provides our first indication of whether collective processes might be important. Finding Debye lengths comparable to the spatial scales doesn't firmly establish a collective plasma effect since it involves interactions between individual particles and not between large groups of particles in the plasma or the plasma as a whole. However, under the presence of collisions, the particles might already behave differently from what would be expected when using a single particle scenario. The vacuum Coulomb force is long range, but in a plasma, this force only extends a Debye length from the source, as a consequence of the Debye shielding cloud (Cravens, 1997, Pg. 37). Although on small scales, a plasma in thermal equilibrium can have significant departures from charge neutrality ($n_e \neq n_i$), for long spatial scales, an equilibrium plasma must maintain charge

neutrality. (quasi-neutrality.)

The size of the Debye length (i.e. shielding cloud) increases as the electron temperature increases because electrons with greater kinetic energy are better able to overcome the Coulomb attraction associated with the potential (in the vicinity of the test charge). On the other hand, the value λ_D is smaller for a denser plasma because more electrons are available to populate the shielding cloud. (And note that the density variation is greater when the electron gas is cold than when the gas is hot).

The Debye length for electrons is defined as (Cravens, 1997, Pg. 37) :

$$\lambda_D = \sqrt{\frac{\epsilon_\circ k_B T_e}{q_e^2 n_e}} \quad \text{(SI)} \tag{6}$$

If I determine that collective effects in a plasma are possible, then a plasma motion that I want to identify is Langmuir oscillations. Langmuir oscillations lead to an oscillation frequency in a fully ionized plasma called the electron plasma frequency ω_e (Baumjohann and Treumann, 1997, Pg. 3). If the quasi-neutrality of the plasma is disturbed by some external force, then, because the electrons are much more mobile than the heavier ions, they are accelerated in an attempt to restore the charge neutrality. Due to their inertia, they will move back and forth around some equilibrium position, resulting in fast collective oscillations around the more massive ions. Note that the electron plasma frequency here, refers to a plasma oscillation, rather than to a propagating wave. The definition of the ion plasma frequency and the electron plasma frequency is (Cravens, 1997, Pg. 94-97):

$$\omega_e = \sqrt{\frac{n_e q_e^2}{\epsilon_\circ m_e}} \quad \omega_i = \sqrt{\frac{n_i q_i^2}{\epsilon_\circ m_i}} \quad \omega_p = \sqrt{\omega_e^2 + \omega_i^2} \quad \omega_d = \sqrt{\frac{n_d q_e^2}{\epsilon_\circ m_d}} \tag{7}$$

However, the electron plasma frequency dominates the total plasma frequency because $m_i >> m_e$, therefore: $\omega_p \approx \omega_e$. Table 4 gives Debye lengths (Eqn. 6) and frequencies (Eqn. 7) for electron/ion ω_p plasma oscillations, and the equivalent dust plasma frequency ω_d. For the latter, I invoke a dust particle mass density 1500 kg-m^{-3}, spherical particle of average radii a seen in the middle panel of Fig. 1, a Jovian streams number density n_d, valid for distance 6 R_J – 2 AU, ranging from 10^{-3} – 10^{-8} m^{-3} (Krüger et al., 2004, Table 10.1). Since $n_d d^3 = 1$, then the intergrain distance d of the dust streams particles, $d = \left(\frac{1}{n_d}\right)^{1/3}$, ranges from 10 – 500 m. Table 4

Now I can check ‘Dust-in-Plasma’: $a \ll \lambda_D < d$ and ‘Dusty Plasma’: $a \ll d < \lambda_D$. From the Debye lengths in Table 4, I see that collective effects might be relevant in the magnetospheric region starting from roughly 10–15 R_J, where the intergrain distance d is about 10 m and the Debye length is 10 m. In other words, outward from 10-15 R_J, in the Jovian magnetosphere, it is possible that I have a “dusty plasma”, rather than a “dust-in-plasma”, therefore more complex frequencies and waves might be seen here.

For more refined checks, I examine selected Galileo orbits which show higher quantities of dust present, in order to check dusty plasma conditions. Table 5 shows seven Galileo orbits: E4, G7, G8, E11, E15, C21, G28, which were chosen from the 1996-2003 mission because they demonstrated a high number of impacts plus a high mean dust impact rate. The fluxes which determined the intergrain distance (d) were average fluxes in which the sensitivity and viewing geometry of the dust detector were accounted, provided by Krüger (2005). The speeds for each location at each Galileo encounter were average speeds calculated via the simulation described in the previous section, and seen in the bottom panel of Fig. 1. The $*$ denotes regions where $d < \lambda_D$, i.e., of possible dusty plasma conditions. Table 5

4 Havnes Parameter P of a Dust Particle Embedded in Jupiter's Plasma

The dimensionless parameter P emerged from the simultaneous solution for the surface potential of an ensemble of grains and the potential of the Maxwellian energy-distributed plasma in which the grains were immersed; given ion and collection currents to the grains from the plasma, as well as photoelectron currents, and assuming that the sum of the charging currents to the dust grain was zero. The solutions for the relative dust potential $(U - V_p)q_e/(k_B T)$ and the plasma potential $(V_p q_e)/(k_B T)$ only depend on the parameter (Havnes et al., 1987):

$$P \equiv \frac{4\pi\epsilon_\circ a}{q_e^2 n_e} n_d k_B T \tag{8}$$

where $\epsilon_\circ$ = the permittivity of free space (8.854 $\times$ 10^{-12} C^2-N^{-1}-m^{-2}), a = the dust grain radius (m), n_d = dust number density (m^{-3}), k_B = the Boltzman constant (1.381 $\times$ 10^{-23} J-K^{-1}), T is the plasma temperature (K) (Table 1), q_e is the charge on the electron (1.602 $\times$ 10^{-19} C), and n_e is the plasma density (m^{-3}) (Table 1).

The Havnes et al. (1990, Fig. 1) solutions represent a general scenario of a distribution of dust particle sizes while in plasmas of different composition. The scenario assumes equilibrium dust potentials and does not include secondary electron emission currents. Earlier works by Havnes and colleagues considered more idealized assumptions for dust cloud geometry, dust particle sizes, and plasma energy distributions, and note that the definition for P in the earlier works such as Goertz (1989) must multiply P by $4\pi\epsilon_\circ/q_e$ in order to match Eqn. (8).

The solutions from Havnes' work do not fit perfectly the charging and dynamics of the Jovian dust streams for several reasons: 1) the secondary electron emission is an important charging process for the dust stream particles, especially in the inner Jovian magnetosphere (Horányi et al., 1997), and 2) the dust stream particles do not have a unique equilibrium potential; Meyer-Vernet (1982) demonstrated that the equilibrium potential from secondary electron emission currents may have multiple roots. Moreover, an equilibrium potential is often not reached for the smallest Jovian dust stream particles, where, for example, a 10 nm sized particle needs 1–5

hours to reach equilibrium potential within the Jovian magnetosphere, which is a significant part of the travel time for an escaping particle Graps (2001).

Nevertheless, the potential solutions and parameter should be reliable ‘enough’ indicators of dusty plasma conditions. In Table 6, I calculate P for the same specific locations in Jupiter’s magnetosphere as Table 5, considering temperature T = T_e, given a dust number density $n_d = (1/d)^{(1/3)}$ from the intergrain distances d in Table 5, and applying the average sizes for each location at each Galileo encounter that were calculated via the simulation described previously, and seen in the middle panel of Fig. 1. Table 6

When the Havnes parameter P is very small, then the grain potential U approaches the Spitzer single-grain value of -2.51 $k_B T_e/q_e$, and the plasma potential V_p is zero. Then the grain can be treated as a test particle and the grain’s charge has a negligible effect on the plasma environment, and on the electric and magnetic fields (Horányi et al., 2004).

The tiny P values in Table 6 indicate no dusty plasma conditions, given the present inputs to the Eqn. (8). The discrepancy between the two methods requires a discussion.

5 Discussion

The minimum requirement for collective effects is the same requirement and expression for the existence of a plasma, where many particles are contained within a Debye sphere (to apply statistics), and for each volume element, the plasma is electrically neutral, but now we are substituting dust particles for (ions, electrons): $(4\pi/3)n_d\lambda_D^3$ (note added in proof). The minimum requirement can be expressed via a ratio of $d/\lambda_D = \kappa$, in Barkan et al. (1994)’s notation, where κ should be < 1. Several locations in some of the Galileo spacecraft orbits satisfy the minimum requirement of a dusty plasma, but the conditions do not satisfy the necessary conditions for collective behavior.

A comparison of the energies of the dust streams and the plasma in which they are embedded point to the main difficulty of the Jovian dust streams displaying collective behavior (note added in proof). The plasma kinetic energies are in the tens to approximately one hundred eV, while the high energies of the dust streams are in the range of a few to hundreds of MeV.

The parameter P is a more sensitive measure of collective behavior by giving the ratio for the charges on the dust compared to the electrons in the plasma. The potential solutions as a function of P (Havnes et al., 1990, Fig. 1) illustrate that collective effects of the dust ensemble occur when the parameter $P \sim 1$, which is when the derivative with respect to P for the relative plasma potential caused by the dust, is at a maximum (note added in proof). At this P, local electric potential differences of order $(k_B T/q_e)$ V can be generated by dust density irregularities. If P is less than one, then the maximum potential difference in the dusty plasma is smaller too

(Goertz, 1989; Havnes et al., 1990). Therefore, if we have maximum collective effects, $P \sim 1$, then the maximum electrostatic potential difference from the plasma given a typical temperature listed in Table 1, 5 eV, is: $[U - V_p]\,(k_B T/q_e)$ = 5 V. Since our calculated P is about 10^{10} smaller than that, and likely smaller within any possible dust density irregularities, the true potential differences will be likely very much smaller than 5 V.

It is useful to vary the dust and plasma number density contained in P and see the physical effects. If the conditions for dust favor collective behavior, then if the dust number density is decreased, the grain charges decrease. Here two effects play a role in opposite directions (Verheest, 2000, Pg. 28): 1) the capacitance of the grains increases, and 2) the mean charge for each grain decreases compared to the equilibrium charge of a single grain. Therefore, an increase in dust density means that the grain ensemble has a larger appetite for electrons, but that the number of available electrons per grain decreases.

If the dust number density remains fixed, then from $n_d Q \sim n_e q_e$ for maximum collective conditions, if the dust charge density $n_d Q$ decreases, then the plasma number density n_e should decrease (and therefore, λ_D increases), as well. I follow with a quantitative example.

The ratio κ (which gives the minimum requirement for a dusty plasma) can trace collective effects if properly compared to the number of charges on the grain $Z_d = Q/q_e$. I calculated Z_d via the indirect measurement of $Q = \langle U \rangle 4\pi\epsilon_\circ \langle a \rangle$, where $\langle U \rangle$ and $\langle a \rangle$ are the average potentials and sizes (output from the dust stream model, Fig. 1, as described previously). The ratio κ, which compares the measured interparticle distance d to the plasma Debye length λ_D, was calculated for each of the seven Galileo orbits at the same six locations, and I show them both in Table 7. In addition, I mark with an asterisk the same locations where the *minimum* requirement for dusty plasma conditions ($\kappa < 1$) is satisfied. Table 7

The values in the table do not correlate the decrease of plasma density with dust charge. Two good locations in which to compare is between 6.2 R_J and 15 R_J, where the plasma density n_e decreases drastically. In orbits E4, G8, and G28, the dust number density n_d is roughly constant at 6.2 R_J and 15 R_J, and the ratios for κ decreases. Yet Z_d increases, not decreases, as it should if there existed collective behavior. Moreover, a charge increase appeared in a region: 20 R_J in orbit G8, where a comparison of Debye length and interparticle distance showed possible dusty plasma conditions. Therefore, while it is useful to know the locations in space and time for the minimum (κ) requirements of possible dusty plasma conditions, P can still be small. To have collective behavior the conditions must be additionally supported by the parameter P closer to unity.

6 Conclusions and Future Directions

A natural laboratory to study electromagnetically-controlled cosmic dust has been provided by the Jovian dust streams and the data from the instruments which were on board the Galileo spacecraft. Given the prodigious quantity of dust poured into the Jovian magnetosphere by Io and its volcanoes resulting in the dust streams, the possibility of dusty plasma conditions exist. To study the possibility, I showed how to distinguish between dust-in-plasma and dusty-plasma and how the Havnes parameter P can be used to support or negate the possibility of collective behavior of the dusty plasma.

The result of applying these tools to the Jovian dust streams reveals mostly dust-in-plasma behavior. In the orbits displaying the highest dust stream fluxes, portions of orbits E4, G7, G8, C21 satisfy the minimum requirements for a dusty plasma. However, the P parameter demonstrates that these mild dusty plasma conditions do not lead to collective behavior of the dust stream particles. This result might be a relief to the modelers who have treated the Jovian dust stream particles as isolated particles in their charging and dynamics calculations during the last decade. Or this result might motivate dust researchers who yearn for collective dusty plasma conditions to look elsewhere in the solar system for their natural laboratories.

These other natural dusty plasma laboratories are conveniently under study now or soon to be studied by other spacecraft. One natural laboratory, the Saturn ring system (with its spokes), has been the prime motivator for dusty plasma studies since the time of the Voyager spacecraft twenty years ago. The Cassini spacecraft in orbit around Saturn since 2004 is well-placed to continue those dusty plasma studies. Not only are the spokes today still the topic of PhD theses, but the active moon Enceladus is providing new dust puzzles. In addition, comet missions such as Stardust in its flyby of comet 81P/Wild 2, and Rosetta, on its way to comet 67P/Churyumov-Gerasimenko, provide the instruments and the dusty plasma source (comets) in which to study the complex interplay between dust and plasma.

Lest we not forget about Io, the most active volcanic dust source in the solar system, the archived Galileo data can give information for Jupiter's magnetic field activity at the same time it can trace the activity of Io's volcanoes. This information might give new views for how the mass-loading from Io influences the Jupiter environment. In future work, I would like to incorporate real-time plasma and magnetic field data with higher resolution DDS dust fluxes in order to continue to understand the Jovian dust streams and the Jupiter plasma and magnetosphere.

Software

A spreadsheet that follows the calculations of this paper can be found at:
http://www.mpi-hd.mpg.de/dustgroup/~graps/dustyplasma/ .

Acknowledgments

I thank Eberhard Grün and Mihaly Horányi for valuable discussions, Harald Krüger for good discussions, feedback and excellent Galileo DDS data support, two anonymous referees for their inestimable and important comments, the Galileo project at JPL for effective and successful mission operations during the Galileo spacecraft's years in orbit, and the INAF Istituto di Fisica dello Spazio Interplanetario for its financial support.

References

Bagenal, F., 1989. Torus-magnetosphere coupling. In: Belton, M., West, R. A., Rahe, J. (Eds.), Time-Variable phenomena in the Jovian system. SP-494. pp. 1–403.

Barkan, A., D'Angelo, N., , Merlino, R. L., 1994. Charging of dust grains in a plasma. Physical Review Letters 73 (23), 3093–3096.

Baumjohann, W., Treumann, R., 1997. Basic Space Plasma Physics. Imperial College Press.

Cravens, T. E., 1997. Physics of Solar System Plasmas. Cambridge University Press.

Goertz, C., 1989. Dusty plasmas in the solar system. Rev Geophys. 27, 271–292.

Graps, A. L., August 1991. Investigating the motions and energies of ions confined in a uniform magnetic field. Master's thesis, San Jose State University.
URL `http://www.amara.com/ftpstuff/MSThesis.pdf`

Graps, A. L., Jul. 2001. Io revealed in the Jovian dust streams. Ph.D. thesis, Ruprecht-Karls-Universität Heidelberg.
URL `http://www.ub.uni-heidelberg.de/archiv/1838`

Graps, A. L., Grün, E., Svedhem, H., Krüger, H., Horányi, M., Heck, A., Lammers, S., 2000. Io as a source of the Jovian dust streams. Nature 405, 48–50.

Grün, E., Baguhl, M., Hamilton, D. P., Riemann, R., Zook, H. A., Dermott, S., Fechtig, H., Gustafson, B. A., Hanner, M. S., Horányi, M., Khurana, K. K., Kissel, J., Kivelson, M., Lindblad, B.-A., Linkert, D., Linkert, G., Mann, I., McDonnell, J. A. M., Morfill, G. E., Polanskey, C., Schwehm, G., Srama, R., May 1996a. Constraints from Galileo observations on the origin of the Jovian dust streams. Nature 381, 395–398.

Grün, E., Hamilton, D. P., Riemann, R., Dermott, S., Fechtig, H., Gustafson, B. A., Hanner, M. S., Heck, A., Horányi, M., Kissel, J., Krüger, H., Lindblad, B.-A., Linkert, D., Linkert, G., Mann, I., McDonnell, J. A. M., Morfill, G. E., Polanskey, C., Schwehm, G., Srama, R., Zook, H. A., 1996b. Dust measurements during the initial Galileo Jupiter approach and Io encounter. Science 274, 399–401.

Grün, E., Krüger, H., Graps, A. L., Hamilton, D. P., Heck, A., Dermott, S., Fechtig, H., Zook, H. A., Gustafson, B. A., Hanner, M. S., Horányi, M., Kissel, J., Lindblad, B. A., Linkert, D., Linkert, G., Mann, I., McDonnell, J. A. M., Morfill, G. E., Polanskey, C., Schwehm, G., Srama, R., Sep. 1997. Dust measurements in the Jovian magnetosphere. Geophys. Res. Letters 24, 2171–2174.

Havnes, O., Aanesen, T. K., Melandsø, F., 1990. On dust charges and plasma po-

tentials in a dusty plasma with dust size distribution. J. Geophys. Res. 95 (A5), 6581–8585.
Havnes, O., Goertz, C., Morfill, G., Grün, E., Ip, W., 1987. Dust charges, cloud potential and instabilities in a dust cloud embedded in a plasma. J. Geophys. Res. 92 (A3), 2281–2287.
Horányi, M., Cravens, T., 1996. The structure and dynamics of Jupiter's ring. Nature 381, 293–295.
Horányi, M., Grün, E., Heck, A., 1997. Modeling the Galileo dust measurements at Jupiter. Geophys. Res. Letters 24, 2175–2178.
Horányi, M., Hartquist, T. W., Havnes, O., Mendis, D. A., Morfill, G. E., Dec 2004. Dusty plasma effects in Saturn's magnetosphere. Reviews of Geophysics 42, RG4002.
Krivov, A. V., Krüger, H., Grün, E., Thiessenhusen, K., Hamilton, D. P., Jan. 2002. A tenuous dust ring of Jupiter formed by escaping ejecta from the Galilean satellites. Journal of Geophysical Research (Planets) 107, 1029–1041.
Krüger, H., 2005. personal communication.
Krüger, H., Horányi, M., Grün, E., Jan. 2003. Jovian dust streams: Probes of the Io plasma torus. Geophys. Res. Letters 30, 1058–1061.
Krüger, H., Horányi, M., Krivov, A., Graps, A., 2004. Jovian dust: Streams, clouds and rings. In: Jupiter: The Planet, Satellites & Magnetosphere. Cambridge University Press, pp. 219–240.
Meyer-Vernet, M., 1982. 'Flip-flop' of electric potential of dust grains in space. Astr. Ap. 105, 98–106.
Spencer, J. R., Schneider, N. M., 1996. Io on the eve of the Galileo mission. Ann. Rev. Earth Sp. Sci. 24, 125–190.
Verheest, F., 2000. Waves in Dusty Space Plasmas. Kluwer.

Table 1
Jupiter Plasma Representative Numbers

Location (R_{J})	T_e (eV)	T_i (eV)	n_e (m^{-3})	avim (a.m.u.)	m_i (kg)
6.2	4.9	60	1.3×10^{9}	22.5	3.7×10^{-26}
8	5.4	60	1.6×10^{8}	19.6	3.2×10^{-26}
10	22.5	100	2.3×10^{7}	17.1	2.8×10^{-26}
15	22.0	120	3.6×10^{6}	15.6	3.7×10^{-26}
20	22.0	120	1.3×10^{6}	15.6	2.6×10^{-26}
30	22.0	120	1.0×10^{6}	15.6	2.6×10^{-26}

R_{J}: distance from the center of Jupiter = 71398 km

T_e: electron temperature, T_i: ion temperature

n_e: electron number density, avim: average ion mass, m_i: ion mass

Table 2
Jupiter Plasma Single Particle Motions Part I

Location (R_{J})	a (m)	$\lvert Q_d \rvert$ (C)	$\langle v_i \rangle$ ($\mathrm{m\text{-}s}^{-1}$)	$\langle v_e \rangle$ ($\mathrm{m\text{-}s}^{-1}$)	$\langle v_d \rangle$ ($\mathrm{m\text{-}s}^{-1}$)
6.2	1.2×10^{-8}	7.3×10^{-18}	2.3×10^{4}	1.3×10^{6}	5.2×10^{4}
8	1.2×10^{-8}	3.3×10^{-18}	2.4×10^{4}	1.4×10^{6}	1.2×10^{5}
10	1.8×10^{-8}	9.1×10^{-18}	3.4×10^{4}	2.8×10^{6}	9.9×10^{4}
15	2.4×10^{-8}	1.5×10^{-17}	3.8×10^{4}	2.8×10^{6}	8.2×10^{4}
20	2.4×10^{-8}	1.5×10^{-17}	3.8×10^{4}	2.8×10^{6}	9.1×10^{4}
30	2.7×10^{-8}	2.0×10^{-17}	3.8×10^{4}	2.8×10^{6}	1.1×10^{5}

Table 3
Jupiter Plasma Single Particle Motions Part II

Location (R_{J})	Ω_i (sec^{-1})	Ω_e (sec^{-1})	Ω_d (sec^{-1})	R_{gi} (m)	R_{ge} (m)	R_{gd} (m)
6.2	7.5	3.1×10^{5}	1.2×10^{-3}	3.0×10^{3}	4.2	4.4×10^{7}
8	4.0	1.4×10^{5}	2.5×10^{-4}	6.0×10^{3}	9.6	4.7×10^{8}
10	2.4	7.4×10^{4}	1.0×10^{-4}	1.4×10^{4}	3.8×10^{1}	9.6×10^{8}
15	7.7×10^{-1}	2.2×10^{4}	2.1×10^{-5}	5.0×10^{4}	1.3×10^{2}	3.9×10^{9}
20	3.2×10^{-1}	9.2×10^{3}	9.3×10^{-6}	1.2×10^{5}	3.0×10^{2}	9.8×10^{9}
30	9.6×10^{-2}	2.7×10^{3}	2.5×10^{-6}	4.0×10^{5}	1.0×10^{3}	4.6×10^{10}

Table 4
Jupiter Plasma Debye Lengths and Frequencies

Location (R_{J})	λ_D (m)	ω_p (s^{-1})	ω_d (s^{-1})
6.2	4.5×10^{-1}	2.0×10^{6}	7.4×10^{-4} – 7.4×10^{-7}
8	1.4	7.0×10^{5}	3.3×10^{-4} – 3.3×10^{-7}
10	7.3	2.7×10^{5}	5.0×10^{-4} – 5.0×10^{-7}
15	1.8×10^{1}	1.1×10^{5}	5.2×10^{-4} – 5.2×10^{-7}
20	3.0×10^{1}	6.4×10^{4}	5.5×10^{-4} – 5.5×10^{-7}
30	3.5×10^{1}	5.6×10^{4}	6.0×10^{-4} – 6.0×10^{-7}

Table 5
Checking Interparticle Distance d for Selected Galileo Orbits

r (R_{J})	E4 d (m)	G7 d (m)	G8 d (m)	E11 d (m)	E15 d (m)	C21 d (m)	G28 d (m)
6.2	1.2×10^{2}	8.0×10^{1}	5.6×10^{1}	1.6×10^{2}	1.2×10^{2}	4.7×10^{1}	1.2×10^{2}
8	5.8×10^{3}	1.0×10^{2}	7.3×10^{1}	2.1×10^{2}	1.6×10^{2}	5.8×10^{1}	1.6×10^{2}
10	4.6×10^{3}	7.9×10^{1}	7.9×10^{1}	1.7×10^{2}	1.3×10^{2}	2.7×10^{1}	1.5×10^{2}
15	3.4×10^{2}	2.2×10^{1}	3.4×10^{1}	7.4×10^{1}	2.9×10^{1}	8.0 *	1.6×10^{2}
20	1.8×10^{2}	2.1×10^{1} *	2.6×10^{1} *	4.5×10^{1}	4.5×10^{1}	7.1 *	1.7×10^{2}
30	3.1×10^{1} *	8.3×10^{1}	3.1×10^{1} *	7.2×10^{1}	9.6×10^{1}	2.8×10^{1} *	2.2×10^{2}

Table 6
Checking Havnes Parameter P for Selected Galileo Orbits

r (R_{J})	E4 P	G7 P	G8 P	E11 P	E15 P	C21 P	G28 P
6.2	1.8×10^{-14}	6.0×10^{-14}	1.8×10^{-13}	7.2×10^{-15}	1.8×10^{-14}	3.0×10^{-13}	1.8×10^{-14}
8	1.5×10^{-15}	2.5×10^{-13}	7.4×10^{-13}	3.0×10^{-14}	7.4×10^{-14}	1.5×10^{-12}	7.4×10^{-14}
10	1.2×10^{-13}	2.4×10^{-11}	2.4×10^{-11}	2.4×10^{-12}	6.1×10^{-12}	6.1×10^{-10}	3.7×10^{-12}
15	2.5×10^{-9}	1.0×10^{-8}	2.5×10^{-9}	2.5×10^{-10}	4.4×10^{-9}	2.0×10^{-7}	2.5×10^{-11}
20	4.9×10^{-8}	3.1×10^{-8}	1.5×10^{-8}	3.1×10^{-9}	3.1×10^{-9}	7.7×10^{-7}	6.2×10^{-11}
30	1.4×10^{-8}	7.2×10^{-10}	1.4×10^{-8}	1.1×10^{-9}	4.7×10^{-10}	1.8×10^{-8}	3.6×10^{-11}

Table 7
Checking If κ Changes With Z_d for Selected Galileo Orbits

r (R_{J})	Z_d	E4 κ	G7 κ	G8 κ	E11 κ	E15 κ	C21 κ	G28 κ
6.2	45	54	36	25	73	54	21	54
8	20	4200	77	53	160	110	42	110
10	57	640	11	11	24	17	3.8	21
15	91	19	1.2	1.9	4.0	1.6	0.43 *	8.7
20	96	5.9	0.69 *	0.87 *	1.5	1.5	0.24 *	5.5
30	120	0.80 *	2.2	0.80 *	1.9	2.5	0.74 *	5.9

Figure Caption

Useful parameters from a simulation of of dust stream particles at 15 hours after release from a radius 6.2 R_J ring. **Top)** Charge potential (in V), **Middle)** Particle size (in nm), and **Bottom)** Speed versus radius from the center of Jupiter in units of Jupiter radius (distance R_J= 71492 km). The (top) charge potential panel illustrates the positive charging of the dust especially near the plasma torus due to the secondary electron emission current (Horányi et al., 1997). The middle panel illustrates the window of ejection sizes (Horányi and Cravens, 1996; Krivov et al., 2002; Graps, 2001), where particles smaller than a particular size gyrate along Jupiter's magnetic field lines and never escape, while particles larger than a particular size are dominated by gravitational forces and unable to escape. The dearth of particle sizes in the middle of the panel are those whose sizes were favorable to ejection from the magnetosphere. The speeds seen in the bottom panel demonstrate that most of the fastest particles particles ($>$ 400 $\mathrm{km\,s^{-1}}$) escaped quickly, a few larger particles ($>$ 20nm), still escaping can be seen scattered in speed in the middle of the figure. The rest of the particles are bound, one population, seen along a steep speed gradient from about 300 $\mathrm{km\,s^{-1}}$ down to 80 $\mathrm{km\,s^{-1}}$, are those that are dominated by Lorentz forces, while the others, along the bottom of the figure that show a gentle speed gradient, are dominated by gravitational forces.

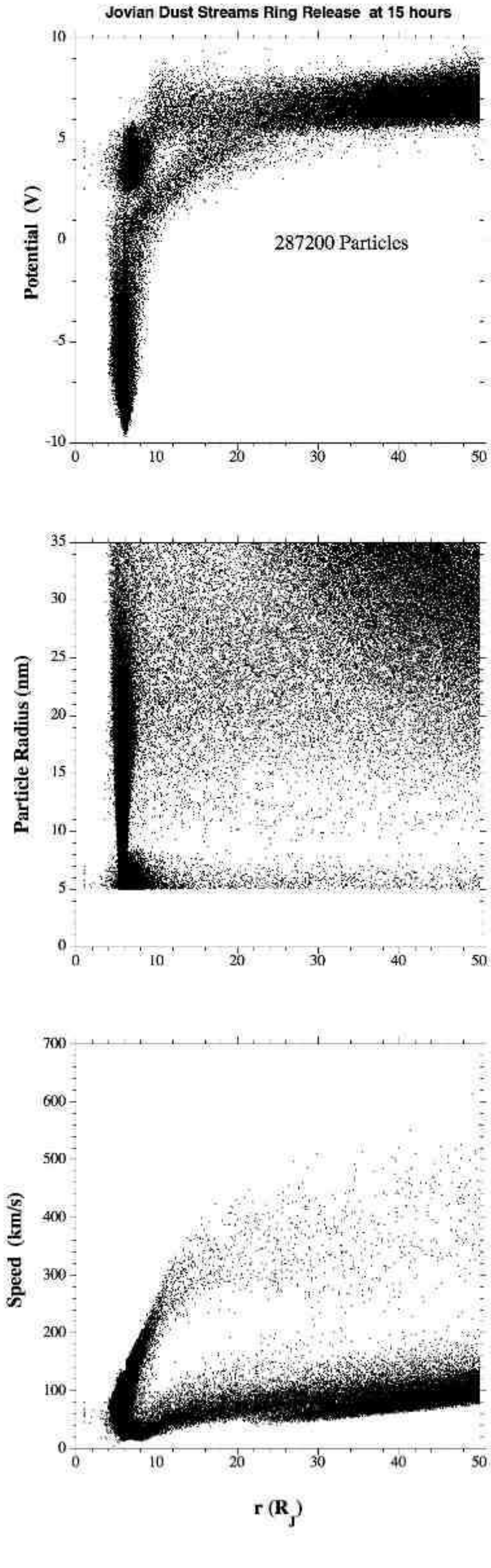
Jovian Dust Streams Ring Release at 15 hours
Potential (V)
287200 Particles
Particle Radius (nm)
Speed (km/s)
r (R_J)